Ultrasonography detects early laryngeal muscle atrophy in an equine neurectomy model

Heather J. Chalmers[*] DVM, PhD, Jeff Caswell[**] DVM, PhD , Justin Perkins BVet Med MS, David Goodwin BSc, Laurent Viel* DVM, PhD, Norm G. Ducharme[***] DVM, MS, Richard J Piercy, MA VetMB, PhD.

Author affiliations:
Department of *Clinical Studies and **Pathobiology
Ontario Veterinary College
University of Guelph
Canada
N1G 2W1
and

***Department of Clinical Sciences
New York State College of Veterinary Medicine
Cornell University
Ithaca, NY, 14853

^Department of Clinical Sciences and Services
Royal Veterinary College
University of London
London, UK

Running title: Ultrasound of laryngeal muscle atrophy

Financial Disclosure: This work was supported by Equine Guelph and MedEl Corporation, Austria.

The authors declare no conflicts of interest.

Corresponding author: Dr. Heather Chalmers, heather.chalmers@uoguelph.ca
c/o Department of Clinical Studies
Ontario Veterinary College
University of Guelph
Guelph, ON
N1G 2W1
519-824-4120 ext 54024

Ultrasonography detects early laryngeal muscle atrophy in an equine neurectomy model

Introduction: A unilateral neurectomy model was used to study the relationship between histologic and ultrasonographic tissue characteristics during muscle atrophy over time.

Methods: *In vivo* experimental study in equine model (n=28). Mean pixel intensity of ultrasonographic images was measured, a muscle appearance grade was assigned weekly, and muscles were harvested from 4-32 weeks. Minimum fiber diameter, fiber density per unit area, percent collagen, percent fat, and fiber type profile were measured from muscle cryosections and correlated with the ultrasonographic parameters.

Results: A significant relationship was identified between collagen content, minimum fiber diameter, and ultrasonographic muscle appearance as early as 8 weeks. There was no apparent association between fat content of muscle and the ultrasonographic appearance of atrophy prior to 28 weeks in this model.

Discussion: Early muscle atrophy prior to fatty infiltration is detectable with ultrasound. The effect of muscle collagen content on echointensity may be mediated by reduced fiber diameter.

Keywords: muscle, atrophy, ultrasound, larynx, histology

Introduction:

Diagnostic imaging modalities are at the forefront of the emerging field of non-invasive tissue characterization and offer expanding potential as a non-invasive way to assess muscle. There is need for detailed study of the relationship between the histologic and ultrasonographic findings of muscle tissue in health and disease. In neuropathic conditions, the ultrasonographic appearance of muscle has been characterized as having increased echogenicity, while with certain myopathies no such change is observed.[1] The reason(s) for altered appearance of muscle under conditions of neurogenic atrophy are understood incompletely. Several authors have hypothesized that the increase in echogenicity is the result of fat and fibrous tissue infiltration.[2-5] Isolated attempts have been made to correlate muscle echogenicity and histologic parameters with mixed results; the relative effects of fat and collagen content have been inconsistent in the models studied.

Muscle biopsy, together with functional assessment tests, genetic testing, and/or electrodiagnosis, is the gold standard diagnostic test for many neuromuscular conditions. However, there are certain clinical situations in which biopsy, direct functional assessment, and electrodiagnosis can be neither practical nor desirable. These include situations where: 1) muscles have limited anatomic access, such as ocular muscles; 2) muscles are very small and make biopsy difficult or excessively invasive; 3) muscles could become unduly scarred by the procedure, thereby influencing muscle function; 4) muscles have already been biopsied and require non-invasive monitoring over time; 5) situations in which electrodiagnostics are undesirable for technical, anatomical, or patient-related reasons. Therefore, the use of non-invasive

testing, such as ultrasonography, to predict muscle tissue composition has broad potential to provide for early diagnosis and long-term monitoring.

In horses, an idiopathic condition termed recurrent laryngeal neuropathy (known as "roaring") with a unilateral clinical presentation is a common disease of the laryngeal muscles.[6-9] In affected animals, primary axonopathy of the recurrent laryngeal nerve leads to secondary neurogenic atrophy and dysfunction of the intrinsic laryngeal muscles. The use of ultrasound to assess the laryngeal muscles in horses has emerged as a more accurate technique than resting functional assessment using upper airway endoscopy for diagnosis.[10-12] Furthermore, the use of quantitative ultrasonography appears to allow stratification of disease severity. Developing this technology as a screening test for roaring in horses, or neuropathic disease in humans, requires expanded understanding of the corresponding histologic alterations that correlate with a change in muscle ultrasonographic appearance.

The aims of this work were: 1) to correlate the ultrasonographic appearance of the intrinsic laryngeal muscles with the histologic characteristics at serial time points following neurectomy and 2) to determine the severity of corresponding histologic lesions necessary for detection of ultrasonographic abnormalities.

We developed 2 hypotheses: 1) the mean pixel intensity of ultrasonographic images of muscle would correlate with 1 or more of the following: mean fiber diameter, fiber density, collagen content per unit area, fat content per unit area, and muscle fiber type; and 2) the muscle appearance grade (a semi-quantitative score) would correlate with 1

or more of the following: mean fiber diameter, fiber density, collagen content per unit area, fat content per unit area, and muscle fiber type.

Materials and Methods:

Subjects

A total of 28 Standardbred horses with a mean age of 4.2 years (range 2-8 years) comprising 17 females and 11 gelded males were included for study. The horses included were free from RLN as determined by resting and exercising upper airway endoscopic examination, normal baseline laryngeal ultrasonographic examination, and lack of clinical signs of roaring. They were assigned in groups of 4 to subgroups based on the length of time following neurectomy: 4 weeks, 8 weeks, 14 weeks, 18 weeks, 24 weeks, 28 weeks, and 32 weeks. The study was approved by the institutional Animal Care and Use Committee of the University of Guelph.

Neurectomy procedure

With horses under general anesthesia, a 2cm section from the mid-cervical region of the right recurrent laryngeal nerve was removed at time = 0. Each cut end of the nerve was ligated with 00 polypropylene suture to prevent axonal regrowth. Upon recovery from general anesthesia, resting upper airway video endoscopy was performed to confirm complete right laryngeal paralysis. Horses were treated post-operatively with 1g phenylbutazone orally twice daily for 3 days and 22mg/kg trimethoprim sulfa orally twice daily for 7 days. Incisions were monitored daily for heat, swelling, pain, or discharge. Skin staples were removed at 14 days.

Ultrasonography

Ultrasonographic imaging was focused on bilateral (left and right sided) assessment of 2 intrinsic laryngeal muscles: the lateral cricoarytenoid (LCA) and the posterior cricoarytenoid (PCA) muscles. Images of the LCA were performed using a GE Logic 5 ultrasound machine (GE Healthcare Inc, Bothell, WA, USA) and 8.5 MHz probe (GE 4-10MHz curvilinear ultrasound probe, GE Healthcare Inc., Bothell, WA, USA),and images of the PCA were obtained using a GE Vivid 9ultrasound machine (GE Healthcare Inc, Bothell, WA, USA) equipped with a pediatric 9 MHz trans-esophageal probe [GE 9T (3-10MHz) pediatric trans-esophageal ultrasound probe, GE Healthcare Inc, Bothell, WA, USA]. For both muscles, the ultrasound examination was performed at baseline (within 24 hours prior to neurectomy surgery) and again prior to sacrifice. Images were obtained using operator-defined individualized gain settings without altering depth, gray map, or power. Additionally, user-optimized images were obtained for each muscle.

Muscle ultrasonographic image analysis

Two methods of ultrasonographic image analysis were used: a semi-quantitative grading scheme, termed the muscle appearance grade, and a quantitative measure of mean pixel intensity. The ultrasound images were converted to JPEG format, randomized, and all identifying data were removed. A previously described muscle appearance grading scheme was applied.[13] The grading scheme consists of grades 1-4 as follows: grade 1, normal muscle appearance as determined by visibility of muscle fiber pattern and isoechoic appearance to ipsilateral thyrohyoid muscle; grade 2, overall slightly increased muscle echogenicity relative to the ipsilateral thyrohyoid muscle;

grade 3, non-uniform heterogenous muscle echogenicity with only slightly increased overall echogenicity; and grade 4, both heterogenous echogenicity and readily apparent overall increase in echogenicity.[13] Ultrasonographic muscle appearance grades were assigned over a 6-week period by an experienced observer (HC) who had knowledge of the project but was blinded to the identity of specific images (neurectomized vs. control side, time since neurectomy). Each image was evaluated 3 times with a minimum of 1 week between observations, and the most commonly assigned grade was used for further analysis. For the quantitative assessment, images were imported into Image Pro Premier (Image Pro Premiere, Media Cybernetics Inc., Rockville, MD, USA), and conversion to gray scale was performed. A standardized, circular region of interest (ROI) was situated over the LCA muscle and PCA muscles. The mean pixel intensity (MPI) and maximum, minimum, and standard deviation of pixel values were recorded.

Muscle histology and image analysis:

Horses were sacrificed at 1 of 7 endpoints with 4 animals in each group: 4, 8, 14, 18, 24, 28, and 32 weeks. Euthanasia was performed using an overdose of barbiturate administered intravenously. Duplicate 5mm diameter cylindrical samples from the LCA muscle and PCA muscles were obtained bilaterally from each horse within 1 hour of euthanasia. For the PCA, samples were obtained from the mid-point of the muscle belly at a site corresponding to the site of transesophageal ultrasound imaging. For the LCA, the sample was obtained from the mid-third of the muscle belly at a site corresponding to the portion of the muscle visualized from the percutaneous lateral ultrasound acoustic window. For each animal, the 4 muscles were aligned on a single cork disc with the

fibers orientated perpendicular to the cork together with a 5mm cube of thyroid tissue to aid in future identification. Samples were then coated with optimal cutting temperature compound (Tissue Tek OCT compound, Sakura Fineteck, CA) and snap frozen in isopentane pre-cooled in liquid nitrogen. The samples were stored at -80^0 C until further processing.

For each horse, serial 8µm cryosections were obtained, air dried onto slides (Superfrost plus microscope slides, Fisher Scientific, Loughborough, UK) and stored at -80^{0}C. For each muscle sample, hematoxylin and eosin (H&E) and oil red O (ORO) stains were performed using routine techniques.[14] Multiple fluorescence labelling to enable fiber typing was performed according to a previously described technique that has been validated for adult equine muscle.[15] Briefly, a goat polyclonal anti-collagen V IgG antibody(1:20) (goat IgG collagen V, Southern Biotechnology, Birmingham, Alabama, USA) diluted in phosphate buffered saline (PBS) was applied to the sections for 60 minutes prior to liberal rinsing in PBS over 5 minutes. Then, an Alexafluor 488 rabbit anti-goat IgG secondary antibody (1:1000) was applied for 60 minutes before further rinsing in PBS. Three different monoclonal mouse IgG antibodies were then used to label all fiber types: slow myosin IgG antibody (slow myosin IgG, MAB1628, Merck Inc, Millipore, UK); type 2a IgG antibody (type 2a IgG, A4.74, Developmental Studies Hybridoma Bank, Iowa, USA); and type 2a and 2x antibody (type 2a and 2x MHCf IgG, NCL-MHCf, Leika, UK). These were individually labelled with Zenon Alexa fluor (Zenon Alexafluor IgG labelling kit, http://www.invitrogen.com)-congugated IgG_1 Fab fragments designed for 3 different emitting wavelengths 350nm (Type1), 594nm (Type 2, all fast), and 647nm (Type2a). The sections were incubated in this mixture for 60 minutes prior

to rinsing, fixed in 4% paraformaldehyde in PBS for 15 minutes, and subsequently mounted (Vectashield mounting medium for fluorescence, Vector Labs, Peterborough UK).

The sections were examined using a fluorescence microscope (Leica DM4000B microscope, Leica Microsystems (UK) Ltd., Buckinghamshire, UK) with filters designed for each of the emitting wavelengths. Slides were examined using an x10 objective, and representative sections typically containing several hundred fibers were selected by an experienced observer. For each muscle, 2 representative images selected at random were captured. In a few cases, cutting or freezing artifact compromised image quality, and the nearest good quality area was chosen after random positioning. The histologic images were then exported (Axiovision software, Leica Microsystems (UK) Ltd., Buckinghamshire, UK) and processed with Volocity software (Volocity software, PerkinElmer, Cambridge, UK) for background correction and conversion into gray scale tagged image file format (TIFF) ready for image analysis. Background correction was conducted with blank images captured with the same objective for each filter block used. QWin Quips image analysis software V3 [QWin Quips image analysis software V3, Leica Microsystems (UK) Ltd., Buckinghamshire, UK] was then used to write a macro to count the fibers and measure the minimum diameter for each fiber derived from the collagen gray scale image that outlined fiber basement membranes. For each muscle from each horse, the mean minimum fiber (Feret) diameter was calculated.[16]

The proportion of lipid within each image was calculated from the ORO-stained sections. Two selected images from each muscle were captured using an Olympus BX41 microscope x10 objective, and TIFF images were exported into Velocity software

(Volocity software, PerkinElmer, Cambridge, UK) for analysis. Color discrimination thresholding was used to identify the orange stain corresponding to the fat within the muscle. A binary image was created and used to measure the pixel area. The percent pixel area of ORO-stained lipid was calculated from the mean value calculated for each image for each muscle total pixel area.

Percent collagen per unit area was calculated from the collagen V immunofluorescence images. Two selected images from each muscle were captured using a Leica microscope (Leica DM4000B microscope, Leica Microsystems (UK) Ltd., Buckinghamshire, UK) x10 objective and AxioVisionsoftware (Leica Microsystems (UK) Ltd., Buckinghamshire, UK). Background correction was performed using Volocity (Volocity software, PerkinElmer, Cambridge, UK) software. The corrected TIFF images were analyzed with Volocity (Volocity software, PerkinElmer, Cambridge, UK) software to discriminate the pixels related to collagen immunolabelling. The percent collagen per unit area was calculated from the mean of the total pixel area of each of the 2 images for each muscle.

Fiber type proportions were determined by manual counting for all horses by examining 2 selected images for each muscle. Each fiber type was identified by the color of the emitting fluorescence that were pseudo-colored by the image analysis software as blue (type 1), orange (type2a), and red (type 2x). The few fibers that were identified as hybrids were assigned to whichever myosin heavy chain isoform was mostly strongly expressed for the fiber. The proportion for each fiber type was then calculated as a percentage of the total number of fibers counted per muscle.

Statistical analysis

The correlations between histologic parameters and ultrasonographic muscle appearance grades were assessed with Spearman correlation coefficients. The relationship of the histologic parameters to ultrasonographic muscle appearance grade was also examined using a generalized linear mixed model, with the histologic outcomes as the dependant variable. Residual analyses were performed to test the model assumptions; these were that the errors were normally distributed, homoscedasticity (equal variance), and independence of errors. The assumption of normality was tested using the 4 tests offered by SAS (Shapiro-Wilk, Kolmogorov-Smirnov, Cramer-von Mises, Anderson-Darling) and plotting of residuals against predicted values. The echo-intensity data were modelled as a generalized linear mixed model, and a logit transform was used because the dependent variable had a finite range (0-255). For all statistical models, the model assumptions were tested, and where necessary, transformations were used to satisfy model assumptions. All analyses were performed using SAS software version 9.2 (SAS Software Inc, Cary, NC, USA), and significance was set at $P<0.05$.

Results

Neurectomy resulted in ultrasonographically-visible muscle atrophy that was minimally apparent at 4 weeks and became progressively more evident at each time point thereafter. When the muscles were examined histologically, signs consistent with neurogenic atrophy identified on the right side included reduced fiber size and increased

connective tissue content (collagen and fat) (Figure 1). A composite image of serial ultrasonographic and corresponding histologic images is shown in Figures 2 and 3.

The observed changes in each histologic parameter over time are shown in Figure 4. Histologically, alteration in minimum fiber diameter was the earliest finding following neurectomy. The earliest time points (weeks 4 and 8) already showed statistically significant alterations in minimum fiber diameter in the right LCA muscle compared to the left LCA muscle (Figure 3A). This was followed closely by significant differences in collagen content between the right and left sides, which were first apparent at 8 weeks post-neurectomy for both the LCA and PCA muscles (P=0.029) (Figure 3B). For fiber density, however, a significant increase was not apparent until 14 weeks post-neurectomy in the right LCA muscle compared to the left (P=0.001) (Figure 3C) and until 18 weeks post-neurectomy in the right PCA muscle compared to the left (P=0.043) (Figure 3C). The alterations in fat content were relatively minor for most of the study period, with some significant differences in fat content between neurectomized and control muscles becoming apparent in the LCA muscle, but not the PCA muscle, late in the study period at 28 weeks (Figure 3D).

Changes in the fiber type profile of the 4 intrinsic laryngeal muscles over time following neurectomy are shown in Figure 5. The fiber types identified included types 1, 2a, and 2x. There were significant differences in the proportion of all 3 fiber types observed when right (neurectomized) and left (control) sides were compared, but fiber type profile did not change as a result of the time horses were neurectomized (Figure5).

The LCA and PCA muscles that had abnormal ultrasonographic muscle appearance grades were noted to exhibit corresponding histologic changes, including significantly reduced minimum fiber diameter, increased fiber density, increased collagen content, and increased fat content compared to muscles that had normal appearance grades. The correlation between ultrasonographic muscle appearance grades and muscle histologic characteristics over time is shown in Table 1. Collagen was the earliest histologic parameter to have a significant correlation with an abnormal muscle appearance grade, which occurred at week 8 and continued to be significantly correlated with muscle appearance grade for all subsequent time points (Table 1). The magnitude of this difference was generally lower than that of minimum fiber diameter (Table 1). Both minimum fiber diameter and fiber density were significantly correlated with muscle appearance grade by week 14. For both parameters, the correlations were strong (Table 1). The fat content of muscle was not significantly correlated with muscle appearance grade until week 28, at which time the correlation was weak (Table 1).

The differences in collagen content, fat content, minimum fiber diameter, and fiber density among the 4 ultrasonographic muscle appearance grades were examined using a mixed model. The odds ratios for all pairwise comparisons between muscle appearance grades are shown in Table 2. Significant differences were noted between all 4 muscle appearance grades for all parameters except fat content (Table 2). The fat content of muscle was only significantly different for muscle appearance grade 4 when compared to all other grades (Table 2).

In addition to the correlations between histological parameters and ultrasound grading, a relationship with the objective ultrasound data of mean pixel intensity was also noted.

Due to the biologic interrelatedness of the parameters of MFD, fiber density, and collagen content, multivariable analysis was necessary to identify which variable(s) remained statistically significant in the most parsimonious model for the objective parameter of mean pixel intensity. Therefore, a generalized linear mixed model was used to relate mean pixel intensity to the various histologic findings. From this, muscle (P=0.0015), and side (P<0.0001) were always significant as main effects and were kept in the model throughout. Gender was not significant and was removed from the model. The histologic parameters tested as independent variables were collagen content, fat content, fiber density, and minimum fiber diameter. A stepwise approach with both forward and backward elimination was used, and due to co-linearity, all pairwise comparisons were tested and were applied to the model in different sequences. Two significant interactions were identified; the interaction of collagen and minimum fiber diameter (P=0.0211) and muscle and minimum fiber diameter (P=0.0028) were both significantly associated with mean pixel intensity. From these various iterations of the generalized linear mixed model, only minimum fiber diameter was significant as a main effect in the model (P=0.0024).

Both the subjective ultrasonographic grading technique and the objective assessment of mean pixel intensity consistently identified atrophy of the laryngeal muscles. The odds of identifying a significant difference between the neurectomized (right) muscles compared to the control (left) side at each time point are listed in Table 3. At the earliest time point of 4 weeks, the odds of the neurectomized (right) LCA being deemed abnormal were significantly higher than the left, as were the odds of the MPI of the right LCA being significantly higher than the left. For the PCA muscle only the objective

measure of MPI was significantly different between the right and left sides. However, for the PCA muscle the odds of the neurectomized (right sided) muscles being graded as abnormal compared to the control (left) side showed a trend towards being significantly at 4 weeks and reached significance at 8 weeks post-neurectomy (Table 3).

Discussion

In this work, the relationship between ultrasonographic appearance of laryngeal muscle and its histologic composition was evaluated at different stages of atrophy in 28 horses following right recurrent laryngeal nerve transection. Both semi-quantitative (muscle appearance grade) and quantitative (mean pixel intensity) measures of muscle echogenicity were found to correlate with key histologic markers of muscle atrophy, most notably, minimum fiber diameter and collagen content per unit area.

The unilateral neurectomy model resulted in complete unilateral laryngeal paralysis on the right side in all horses as observed endoscopically. The corresponding histologic alterations in the right intrinsic laryngeal muscles (compared to those of the left side) included reduced minimum fiber diameter, increased collagen content, increased fiber density, and as a later change, increased fat content. These findings are similar to those reported in horses with recurrent laryngeal neuropathy, which has been characterized to involve progressive alterations in fiber diameter and deposition of fibrous connective tissue and fat.[8] In contrast to clinically affected horses, this model had uniform fiber atrophy, while in horses affected with recurrent laryngeal neuropathy there is a mixed denervation-reinnervation process which results in greater fiber size

variation until end stage disease.[8] Based on our findings, we conclude that there is little to no correlation between fat content and the ultrasonographic characteristics of neurogenic atrophy of laryngeal muscles in the time frames examined. Yet, in other models of muscle disease, fat content correlated significantly with muscle echo-intensity.[3] The differences between previous studies and our results might be due to different stages of disease within the muscle, the uniformity of the denervation, the resistance to denervation of respiratory muscles, and/or different underlying disease processes. The lack of correlation between fat content and muscle ultrasound characteristics in this study might also be because of the low amount of fatty deposition. The identification of significant differences in the ultrasonographic parameters prior to onset of fatty deposition confirms that other key tissue characteristics affect muscle echogenicity. This result might have particular relevance to assessment of neuromuscular conditions with minimal fatty deposition, especially in early disease stages.

The finding that increased collagen content was the earliest tissue parameter that correlated with ultrasonographic changes in muscle should be interpreted with caution. The concept that atrophied muscle has increased collagen content is widely accepted, yet what is less clear is whether this represents *de novo* collagen being added to muscle tissue in response to atrophy or existing collagen becoming a more predominant component of tissue due to a reduction in myofiber size. It is likely a combination of these factors, and substantial inter-relationships between minimum fiber diameter, collagen content, and fiber density exist. Specifically, both minimum fiber diameter and collagen content may reasonably be expected to change together, because a reduction

in minimum fiber diameter would be expected to increase collagen content per unit area even if *de novo* collagen was not synthesized. Similarly, fiber density will increase as minimum fiber diameter decreases. Therefore, minimum fiber diameter, fiber density, and collagen content may act in concert to affect muscle echointensity. Interestingly, minimum fiber diameter, but neither collagen nor fiber density, was found to be a significant main effect when the outcome of echointensity was modelled statistically. When all possible interactions between the histologic variables were tested, collagen was only found to affect muscle echointensity through its interaction with minimum fiber diameter. Minimum fiber diameter has not been assessed as a predictor of muscle echogenicity in the past. Therefore, the concept that an increase in muscle echogenicity is more attributable to changes in fiber size than actual collagen content is a new finding. It is unclear if this is a unique feature of laryngeal muscles or whether it could be applied more broadly in other skeletal muscles. We speculate that observed increases in muscle echogenicity accompanying progressive muscle atrophy may be due to an increase in the number of acoustic barriers encountered by the ultrasound beam when it traverses muscle with reduced fiber diameter.

The finding of early changes in semi-quantitative ultrasound parameters (muscle appearance grade) occurring concurrently with the changes in subjective ultrasound parameters (mean pixel intensity) was somewhat unexpected. Previous work has touted the strengths of quantitative ultrasound, concluding that quantitative means offer superior sensitivity and specificity in differentiating normal from diseased muscle.[17-19] Previous reports of muscle grading with ultrasound have used a scheme described by Heckmatt.[2] This method is limited, because it emphasizes muscle brightness and does

not take other aspects of muscle appearance into consideration. In particular, heterogeneity and echo-texture were not assessed. Furthermore, the Heckmatt scheme uses the long bone echo as a referent for the entire scale; grades are assigned as the long bone echo becomes increasingly less apparent. This limits the clinical application to anatomic locations in which a bone echo is present on the image. Furthermore, it is possible that muscle appearance could be altered without disruption of the underlying bone echo, especially where the muscle becomes more heterogenous without necessarily having an overall increased reflectivity/echogenicity. Based on these limitations, we developed a novel grading scheme for laryngeal muscle neurogenic atrophy. The fact that this system was tailored to detect the spectrum of findings we have come to expect in equine laryngeal muscle atrophy might explain its superior performance. Yet, if the muscle appearance grade is an appropriate substitute for the quantitative measure of mean pixel intensity, then it could be expected that suitable grading schemes could be developed for other important neuromuscular conditions. Grading schemes are more flexible than quantitative measures, because they do not require equipment standardization. Grading systems are also faster, as the muscle can be graded during the examination process without the need to export images and utilize additional software.

Some limitations of methodology used here are evident. Samples were collected at approximately 4 week intervals. Therefore, changes occurring on a timeline that is shorter than 4 weeks were not captured in these data. Furthermore, each group consisted of 4 individuals. Thus it is possible that the study is underpowered to identify

certain changes, and areas where no significant differences were identified should be interpreted with caution.

In conclusion, the ultrasonographic appearance of muscle is affected primarily by mean fiber diameter and concurrently by collagen content in this model. Even in the absence of fatty infiltration, ultrasonographically-detectable changes exist in muscle. Both muscle appearance grade and mean pixel intensity are effective means of identifying muscle neurogenic atrophy. When considering the ability to detect subclinical muscle disease, ultrasonography offers promise as a screening test for early neuropathic change. Ultrasound is an ideal screening tool, as it is highly accessible, without risk to the patient, low cost, and can be performed by a variety of operators. These findings reinforce the strong potential of ultrasonography for assessing muscle in health and disease for veterinary and human medical applications.

List of abbreviations:

H&E – hematoxylin and eosin

LCA – lateral cricoarytenoid muscle

ORO – oil red o

PBS – phosphate buffered saline

PCA – posterior cricoarytenoid muscle

TIFF – tagged image file format

References:

1. Pillen S, Tak RO, Zwa1. Pillen S, Tak RO, Zwarts MJ, Lammens MM, Verrijp KN, Arts IM, et al. Skeletal muscle ultrasound: correlation between fibrous tissue and echo intensity. Ultrasound Med Biol 2009; 35:443-446.

2. Heckmatt J, Leeman S, Dubowitz V. Ultrasound imaging in the diagnosis of muscle disease. J Pediatr 1982; 101:656-660.

3. Reimers K, Reimers CD, Wagner S, Paetzke I, Pongratz DE. Skeletal muscle sonography: a correlative study of echogenicity and morphology. J Ultrasound Med 1993; 12:73-77.

4. Walker FO. Neuromuscular ultrasound. Neurol Clin 2004; 22:563-90, vi.

5. Walker FO, Cartwright MS, Wiesler ER, Caress J. Ultrasound of nerve and muscle. Clin Neurophysiol 2004; 115:495-507.

6. Cahill JI, Goulden BE. Equine laryngeal hemiplegia. Part I. A light microscopic study of peripheral nerves. N Z Vet J 1986; 34:161-169.

7. Cahill JI, Goulden BE. Equine laryngeal hemiplegia. Part II. An electron microscopic study of peripheral nerves. N Z Vet J 1986; 34:170-175.

8. Cahill JI, Goulden BE. Equine laryngeal hemiplegia. Part III. A teased fibre study of peripheral nerves. N Z Vet J 1986; 34:181-185.

9. Cahill JI, Goulden BE. Equine laryngeal hemiplegia. Part IV. Muscle pathology. N Z Vet J 1986; 34:186-190.

10. Chalmers H, Cheetham J, Mohammed H, Yeager A, Ducharme N. Ultrasonography as an aid in the diagnosis of recurrent laryngeal neuropathy in horses. Proc ACVS Symposium 2006:3-4.

11. Chalmers H, Cheetham J, Yeager A, Ducharme N. Ultrasonography of the equine larynx. Vet Radiol Ultrasound 2006; 41:476-481.

12. Garrett K, Woodie J, Embertson R. Association of treadmill upper airway endoscopic evaluation with results of ultrasonography and resting upper ariway endoscopic evaluation. Equine Vet J 2011; 43:365-371.

13. Chalmers HJ, Viel L, Caswell JL, Ducharme N. Ultrasonographic detection of early atrophy of the intrinsic laryngeal muscles of horses. Am J Vet Research 2015; 76:426-36.

14. Dubowitz V, Sewery C. Muscle Biopsy: A practical approach. Saunders Elseiver: London, UK; 2007.

15. Tulloch LK, Perkins JD, Piercy RJ. Multiple immunofluorescence labelling enables simultaneous identification of all mature fibre types in a single equine skeletal muscle cryosection. Equine Vet J 2011; 43:500-503.

16. Briguet A, Courdier-Fruh I, Foster M, Meier T, Magyar JP. Histological parameters for the quantitative assessment of muscular dystrophy in the mdx-mouse. Neuromuscul Disord 2004; 14:675-682.

17. Fjordbakk CT, Revold T, Goodwin D, Piercy RJ. Histological assessment of intrinsic laryngeal musculature in horses with dynamic laryngeal collapse. Equine Vet J 2014; Sep 25. doi: 10.1111/evj.12357.17.

18. Nijboer-Oosterveld J, Van Alfen N, Pillen S. New normal values for quantitative muscle ultrasound: obesity increases muscle echo intensity. Muscle Nerve 2011; 43:142-143.

19. Pillen S, Scholten RR, Zwarts MJ, Verrips A. Quantitative skeletal muscle ultrasonography in children with suspected neuromuscular disease. Muscle Nerve 2003; 27:699-705.

20. Scholten RR, Pillen S, Verrips A, Zwarts MJ. Quantitative ultrasonography of skeletal muscles in children: normal values. Muscle Nerve 2003; 27:693-698.

rts MJ, Lammens MM, Verrijp KN, Arts IM, et al. Skeletal muscle ultrasound: correlation between fibrous tissue and echo intensity. Ultrasound Med Biol 2009; 35:443-446.

2. Heckmatt J, Leeman S, Dubowitz V. Ultrasound imaging in the diagnosis of muscle disease. J Pediatr 1982; 101:656-660.

3. Reimers K, Reimers CD, Wagner S, Paetzke I, Pongratz DE. Skeletal muscle sonography: a correlative study of echogenicity and morphology. J Ultrasound Med 1993; 12:73-77.

4. Walker FO. Neuromuscular ultrasound. Neurol Clin 2004; 22:563-90, vi.

5. Walker FO, Cartwright MS, Wiesler ER, Caress J. Ultrasound of nerve and muscle. Clin Neurophysiol 2004; 115:495-507.

6. Cahill JI, Goulden BE. Equine laryngeal hemiplegia. Part I. A light microscopic study of peripheral nerves. N Z Vet J 1986; 34:161-169.

7. Cahill JI, Goulden BE. Equine laryngeal hemiplegia. Part II. An electron microscopic study of peripheral nerves. N Z Vet J 1986; 34:170-175.

8. Cahill JI, Goulden BE. Equine laryngeal hemiplegia. Part III. A teased fibre study of peripheral nerves. N Z Vet J 1986; 34:181-185.

9. Cahill JI, Goulden BE. Equine laryngeal hemiplegia. Part IV. Muscle pathology. N Z Vet J 1986; 34:186-190.

10. Chalmers H, Cheetham J, Mohammed H, Yeager A, Ducharme N. Ultrasonography as an aid in the diagnosis of recurrent laryngeal neuropathy in horses. Proc ACVS Symposium 2006:3-4.

11. Chalmers H, Cheetham J, Yeager A, Ducharme N. Ultrasonography of the equine larynx. Vet Radiol Ultrasound 2006; 41:476-481.

12. Garrett K, Woodie J, Embertson R. Association of treadmill upper airway endoscopic evaluation with results of ultrasonography and resting upper ariway endoscopic evaluation. Equine Vet J 2011; 43:365-371.

13. Chalmers HJ, Viel L, Caswell JL, Ducharme N. Ultrasonographic detection of early atrophy of the intrinsic laryngeal muscles of horses. Am J Vet Research 2015; 76:426-36.

14. Dubowitz V, Sewery C. Muscle Biopsy: A practical approach. Saunders Elseiver: London, UK; 2007.

15. Tulloch LK, Perkins JD, Piercy RJ. Multiple immunofluorescence labelling enables simultaneous identification of all mature fibre types in a single equine skeletal muscle cryosection. Equine Vet J 2011; 43:500-503.

16. Briguet A, Courdier-Fruh I, Foster M, Meier T, Magyar JP. Histological parameters for the quantitative assessment of muscular dystrophy in the mdx-mouse. Neuromuscul Disord 2004; 14:675-682.

17. Fjordbakk CT, Revold T, Goodwin D, Piercy RJ. Histological assessment of intrinsic laryngeal musculature in horses with dynamic laryngeal collapse. Equine Vet J 2014; Sep 25. doi: 10.1111/evj.12357.17.

18. Nijboer-Oosterveld J, Van Alfen N, Pillen S. New normal values for quantitative muscle ultrasound: obesity increases muscle echo intensity. Muscle Nerve 2011; 43:142-143.

19. Pillen S, Scholten RR, Zwarts MJ, Verrips A. Quantitative skeletal muscle ultrasonography in children with suspected neuromuscular disease. Muscle Nerve 2003; 27:699-705.

20. Scholten RR, Pillen S, Verrips A, Zwarts MJ. Quantitative ultrasonography of skeletal muscles in children: normal values. Muscle Nerve 2003; 27:693-698.

Table 1. Relationship between ultrasonographic muscle appearance grades (1-4) of the intrinsic laryngeal muscles and various histologic parameters at 7 time points following neurectomy, expressed as Spearman correlation coefficients followed by the *P*-values. Signficant comparisons are indicated by *. (MFD= minimum fiber diameter).

Week	Fat	Collagen	MFD	Fiber density
4	0.071 *P*=0.794	0.257 *P*=0.336	-0.451 *P*=0.08	0.413 0.1112
8	-0.109 *P*=0.688	0.614* *P*=0.011	-0.453 *P*=0.078	0.327 *P*=0.2165
14	0.159 *P*=0.556	0.739* *P*=0.001	-0.8135* *P*=0.0001	0.8* *P*=0.0002
18	-0.021 *P*=0.92	0.813* *P*<0.0001	-0.841* *P*<0.0001	0.623* *P*=0.01
23	-0.129 *P*=0.632	0.707* *P*=0.002	-0.797* *P*=0.0002	0.726* *P*=0.002
28	0.515* *P*=0.041	0.868* *P*<0.0001	-0.868* *P*<0.0001	0.759* *P*=0.0006
32	0.434* *P*=0.092	0.786* *P*=0.0003	-0.841* *P*<0.0001	0.868* *P*<0.0001
Overall	0.267* *P*=0.004	0.702* *P*<0.0001	-0.773* *P*<0.0001	0.707* *P*<0.0001

Table 2 The odds ratio (OR) for various histologic parameters between pairwise comparisons of ultrasonographic muscle appearance grades. Significant differences are indicated by *.

Comparison	Collagen	Fat	minimum fiber diameter
Grade 1 vs. 2	OR= 0.782* (0.616, 0.993) *P*=0.044	OR=1.03 (0.528, 2.012) *P*=0.928	OR= 1.417* (1.147, 1.75) *P*=0.002
Grade 1 vs. 3	0.563* (0.47, 0.673) *P*<0.0001	0.975 (0.579, 1.64) *P*=0.9230	1.99* (1.7, 2.324) *P*<0.0001
Grade 1 vs. 4	0.422* (0.338, 0.528) *P*<0.0001	0.28* (0.156, 0.506) *P*<0.0001	2.547* (2.1, 3.09) *P*<0.001
Grade 2 vs. 3	0.719* (0.5486, 0.942) *P*=0.0172	0.946 (0.447, 1.997) *P*=0.8825	1.4* (1.102, 1.787) *P*=0.0066
Grade 2 vs. 4	0.54* (0.390, 0.746) *P*=0.0003	0.272* (0.12239, 0.60628) *P*=0.0018	1.794* (1.35, 2.392) *P*=0.0001
Grade 3 vs. 4	0.751* (0.569, 0.99) *P*=0.0425	0.288* (0.145, 0.568) *P*=0.0005	1.281* (1.006, 1.629) *P*=0.0440

Table 3: Odds of identifying a difference between right and left PCA and LCA muscles at serial time points following right sided neurectomy using the mean pixel intensity (MPI) and the muscle appearance grade (grade). The data are presented as odds ratio, with 95% CI (in parentheses) and *P*-values below, significant odds ratios are indicated by an *

Week	LCA muscle MPI	LCA muscle grade	PCA muscle MPI	PCA muscle grade
0	1.01 (0.76, 1.32) *P*=0.268	1.06 (0.72, 1.18) *P*=0.672	0.92 (0.82, 1.07) *P*=0.173	0.58 (0.01, 25.22) *P*= 0.775
4	1.43* (1.21, 1.69) *P*<0.001	10.21* (5.03, 20.71) *P*<0.0001	1.21* (1.09, 1.35) *P*=0.005	11.43 (0.98, 133.76) *P*=0.052
8	1.98* (1.72, 2.29) *P*<0.0001	64.42* (33.5, 123.9) *P*<0.0001	1.46* (1.32, 1.61) *P*<0.0001	500.8* (62.8, 4026.66) *P*<0.001
14	2.78* (2.39, 3.16) *P*<0.0001	262.52* (114.93, 599.64) *P*<0.0001	1.75* (1.58, 1.95) *P*<0.0001	1084.85* (44.45, 2640.78) *P*<0.001
18	3.81* (3.26, 4.44) *P*<0.0001	690.69* (264.69, 937.46) *P*<0.0001	2.03* (1.81, 2.29) *P*<0.0001	4944.62* (315.25, 77556) *P*<0.001
24	7.36* (5.85, 9.1) *P*<0.0001	1286.55* (3366.85, 4914.76) *P*<0.0001	2.53* (2.18, 2.95) *P*<0.0001	5512.82* (277.91, >999) *P*<0.001
28	10.1* (7.75, 13,16) *P*<0.0001	910.78* (137.41, 6037.22) *P*<0.0001	2.93* (2.45, 3.51) *P*<0.0001	1084.85* (44.47, 26460) *P*<0.001
32	14.0* (10.31, 19.08) *P*<0.0001	416.29* (26.349, 6577.43) *P*<0.0001	3.53* (2.85, 4.37) *P*<0.0001	37.18* (0.330, 4194.15) *P*<0.001

Figure legends:

Figure 1: Representative (x 20 objective) paired images of equine LCA muscles. A. Left and B. Right, LCA fiber typing at 14 weeks following right denervation. C. Left and D. Right LCA, collagen immunohistochemistry at 14 weeks following right denervation. E. Left and F. Right LCAOil red O staining at 22 weeks following right denervation.

Figure 2. Comparative ultrasonographic images of control (left) and neurectomized (right) intrinsic laryngeal muscles at 18-weeks following right recurrent laryngeal neurectomy. Percutaneous ultrasonographic image of (A) the left (control) LCA muscle and transesophageal ultrasonographic image of (C) the left PCA muscle; the muscles have normal echogenicity, and muscle margins are indicated by white dashes on each image. Percutaneous ultrasonographic image of (B) the right (neurectomized) LCA muscle and (D) transesophageal ultrasonographic image of the right PCA muscle, depicting increased echogenicity compared to the control side.

Figure 3: Composite histologic images(x20 objective; H&E) of the same 4 intrinsic laryngeal muscles depicted in Figure 2. The samples were obtained at 18-weeks after right recurrent laryngeal neurectomy and were collected within 24 hours of the ultrasound images in Figure 2. (A) left PCA, (B) left LCA, (C) right PCA, (D) right LCA.

Figure 4: Alterations of intrinsic laryngeal muscles following right neurectomy (n=4 per group). Left PCA (dark blue, control), left LCA (light blue, control), right PCA (dark red, surgery), right LCA (light red/pink, surgery) muscles. (A) Alterations in mean fiber

diameter (MFD) over time. A significant decrease in MFD was observed in the right PCA (*P*=0.001) and LCA (*P*=0.015) muscles beginning at 4 weeks post-neurectomy and remaining significant for all subsequent time points. (B) Alterations in percent (%) collagen per unit area over time. A significant increase in collagen was observed in the right PCA (*P*=0.029) and LCA (*P*=0.029) muscles beginning at 8 weeks post-neurectomy. (C) Alterations in muscle fiber density (expressed as number of fibers per 10x objective) over time. A significant increase in fiber density was observed in right LCA (*P*=0.001) muscles beginning at 14 weeks post-neurectomy. A significant increase in fiber density was observed in right PCA (*P*=0.043) muscles beginning at 18 weeks post-neurectomy. (D) Alterations in fat per unit area (expressed as a percentage) over time. A significant increase in fat content was observed in the right LCA (*P*=0.009) muscles beginning at 28 weeks post-neurectomy

Figure 5. Fiber type profile expressed as the mean of each fiber type percentage within the total sample of 4 different intrinsic laryngeal muscles over time following right recurrent laryngeal neurectomy. Each graph within the composite represents a single muscle. (A) left PCA, (B) right PCA, (C) left LCA, (D) right LCA. The 3 observed fiber types detected include fiber type I (black), fiber type 2x (light gray), and fiber type 2a (gray). Significant differences exist between the right (neurectomized) and left (control) sides, seen as a greater proportion of for fiber type 1 (*P*<0.0001) and a reduction of fiber types 2x (*P*=0.021), and 2a (*P*=0.027). Significant differences exist between PCA and LCA muscles, seen as a greater proportion of fiber type 1 (*P*=0.014) and a lesser

proportion of fiber type 2a (P=0.028), but no significant differences were identified between PCA muscle and LCA muscles for fiber type 2x (P=0.714).

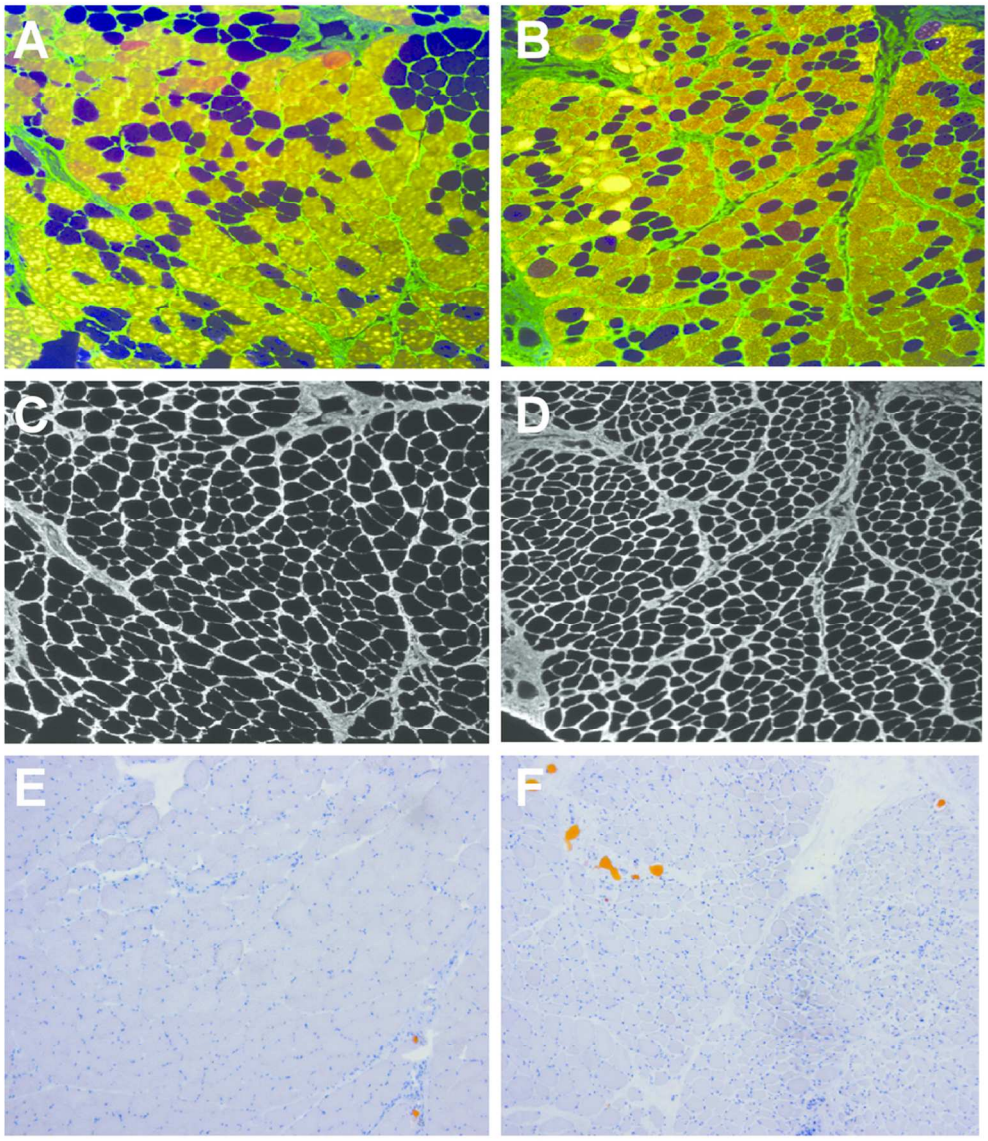

95x109mm (300 x 300 DPI)

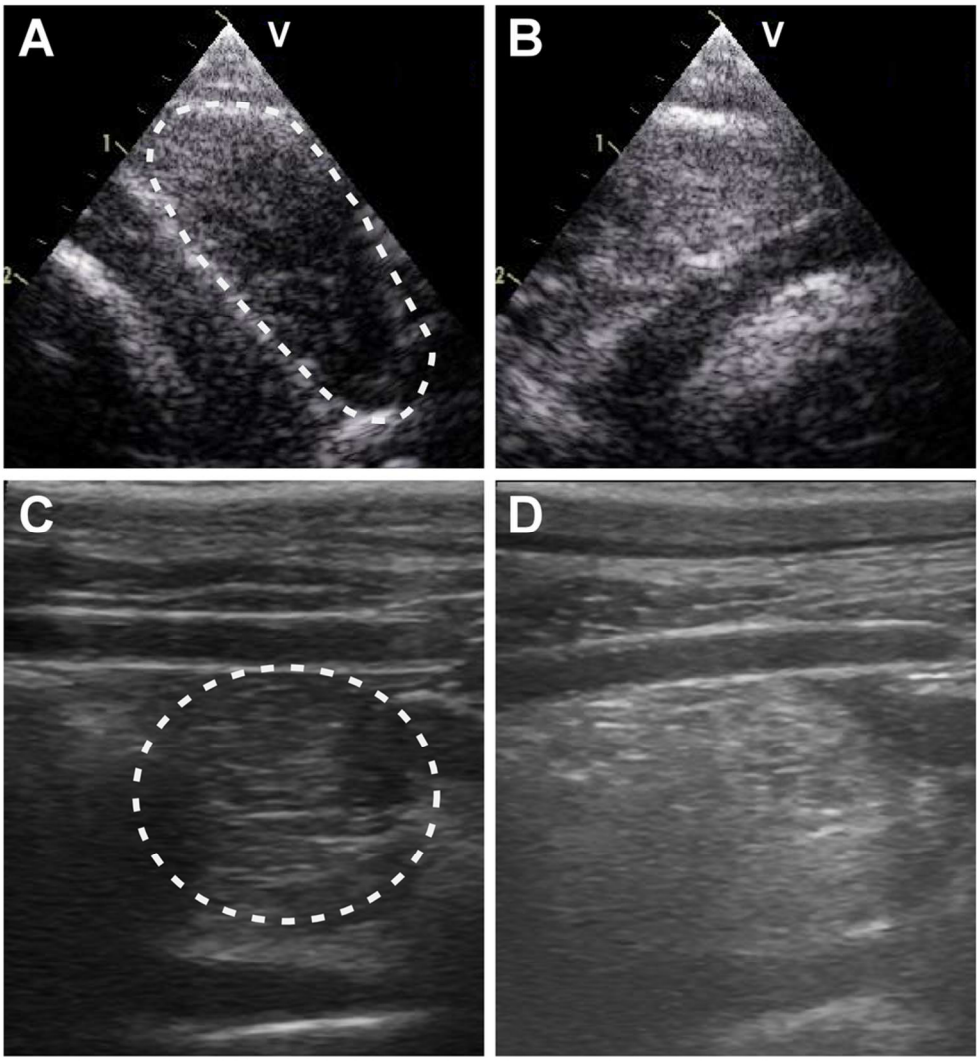

88x94mm (300 x 300 DPI)

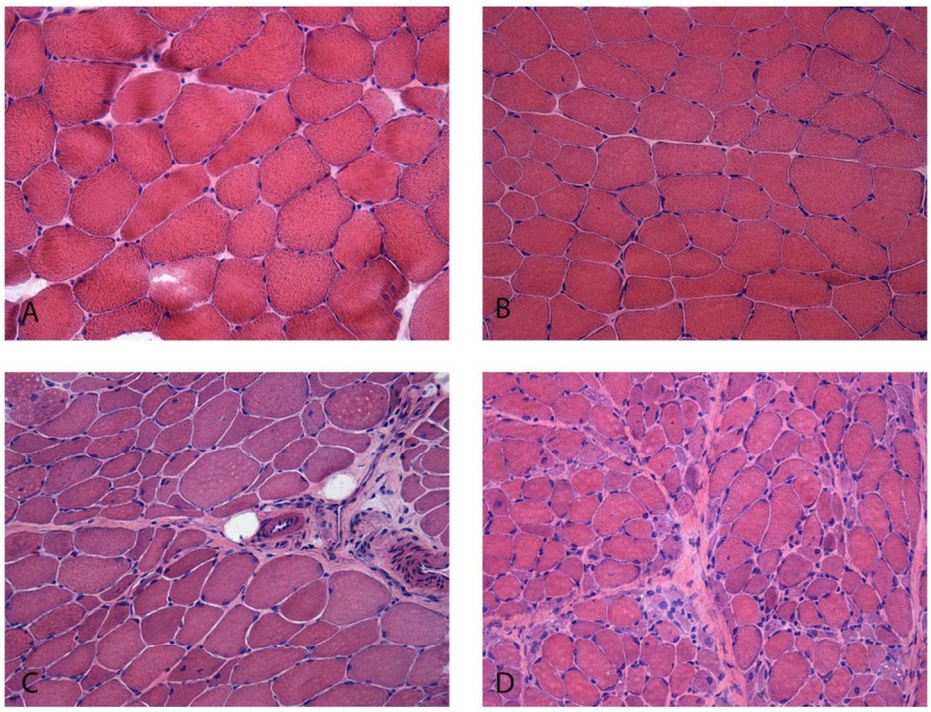

135x104mm (220 x 220 DPI)

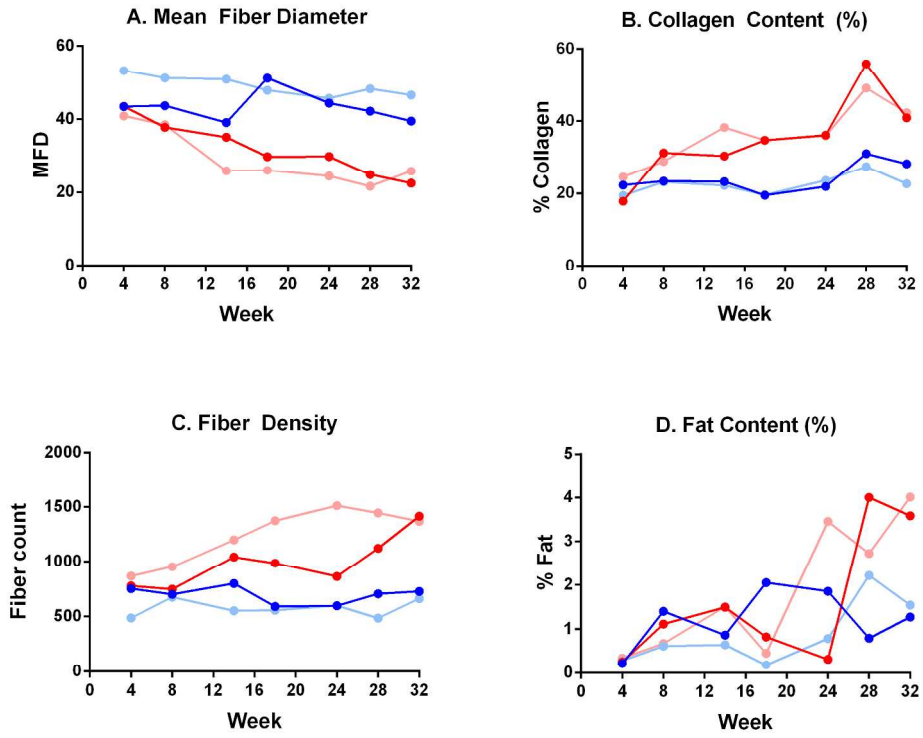

237x187mm (300 x 300 DPI)

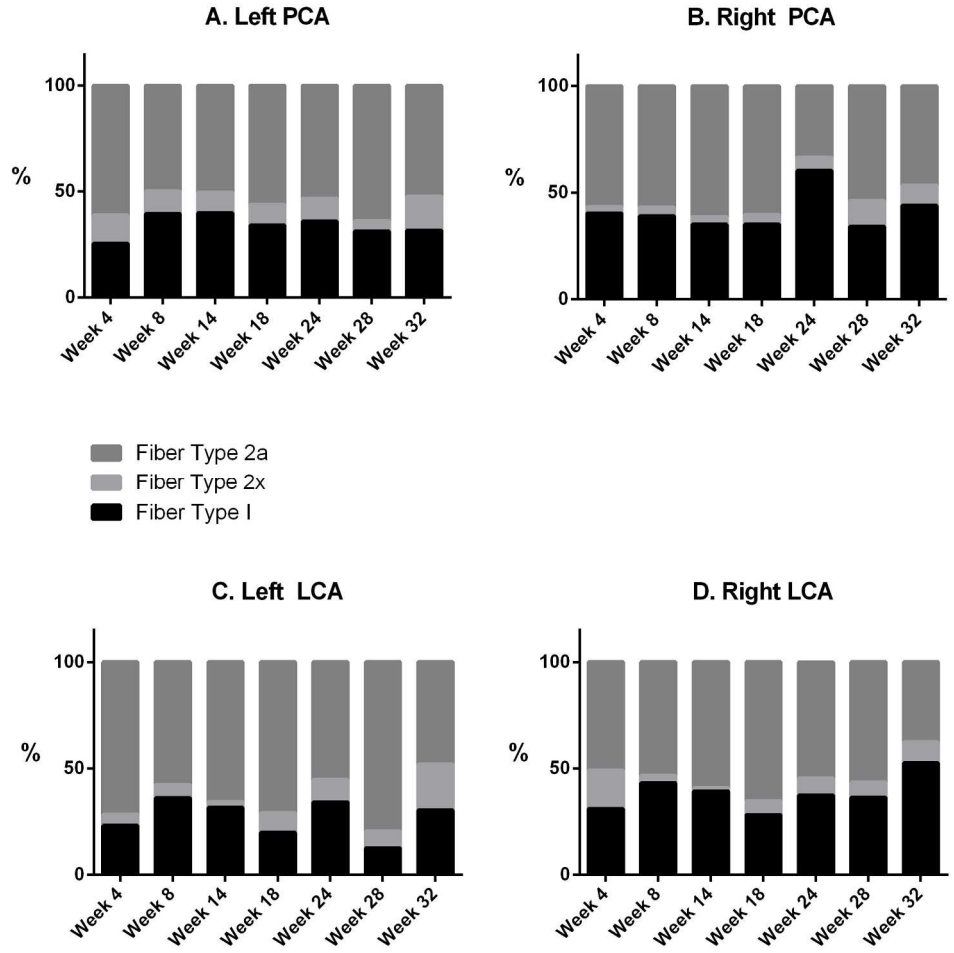

196x199mm (300 x 300 DPI)